

STUDY OF TWO-PHASE PIPE FLOW USING THE AXIAL WIRE-MESH SENSOR

A. Ylönen and J. Hyvärinen

LUT School of Energy Systems / Nuclear Engineering

Lappeenranta University of Technology (LUT)

P.O. Box 20

FI-53851 Lappeenranta, FINLAND

arto.ylonen@lut.fi; juhani.hyvarinen@lut.fi

ABSTRACT

Over the last decade, the Wire-Mesh Sensor (WMS) has become the state-of-the-art method for the measurement of the single-phase mixing and the two-phase flows in high resolution. Typically, the WMSs installed in the pipes and the ducts have been aligned to cover the cross-section of the flow area. The traditional approach would not be ideal if the scope of the study is to measure the development or the dynamics of the flow in the axial direction. Hence, the axially-aligned conductivity Wire-Mesh Sensor was designed and constructed to the centerline of the 50 mm pipe in the current study.

It was foreseen that the axial sensor would give the new insight in the behavior of the two-phase flow. The advantage of such a sensor compared to the cross-sectional sensor is that it is aligned to the same direction in which the flow is also developing. The flow can be measured with the high frequency up to 10 000 frames/s (16×128 wires). The wires were spaced uniformly to form a measurement grid of 2048 cross-points that has the spatial resolution of 3×3 millimeters.

The sensor was tested in an adiabatic HIPE test loop (= Horizontal and Inclined Pipe flow Experiments) that enables the study of the two-phase flow in a pipe at the different inclinations (from horizontal to vertical). A series of two-phase flow experiments was conducted to study the applicability of the sensor and the two-phase flow dynamics in a pipe.

KEYWORDS

Wire-Mesh Sensor, Axial sensor, Two-phase flow, HIPE

1. INTRODUCTION

Single- and two-phase flows in pipes and channels have been studied extensively since the early days nuclear era. The Wire-Mesh Sensor (WMS) measurement technique was developed in the late '90s to offer a new possibility for the measurement of the mixing and the two-phase flow dynamics [1]. Since then the technique has become the state-of-the-art method and has been widely applied for various flow studies, such as recently for the single- and two-phase measurements in a rod bundle [2, 3]. Also, new sensor applications have been developed that are based on the principles of the WMS data acquisition [4, 5]. The use of the WMS technique and the related sensors have enabled the flow studies with the new level of detail in a spatial and a temporal sense. However, typically, the sensors installed in the pipes and the channels have been aligned to cover the cross-section of the flow area. Previously, the stream-wisely aligned "wall-type" sensor has been used in the plenum-type test facility (FLORIS) [6] and in the reactor

pressure vessel test facility (ROCOM) [7] for the mixing studies. The current research examines the possibility of using a sensor that has been aligned to the flow direction at the centerline of the channel. This type of sensor alignment has some clear advantages, but also new types of disadvantages. Next, we present an axial sensor design and the very first results from the two-phase flow measurements in a vertical pipe.

2. EXPERIMENTAL SET-UP

The test facility and the sensor used for the measurements presented in this paper are described next. The adiabatic test loop (HIPE) was constructed to study various two-phase flows in an inclined pipe. The test facility is also applied for the educational purposes as the transparency of the flow channel allows the students to observe the different two-phase flow phenomena.

2.1. The HIPE Test Facility

The new test facility was designed to support the experimental activities related to the advanced measurement techniques. The test facility is also the first one with the wire-mesh sensors in LUT and Finland. The facility has a transparent test section (Acrylic pipe with the inside diameter of 50 mm), whose alignment can be arbitrarily changed between the vertical and the horizontal, hence it is called as the HIPE (=Horizontal and Inclined Pipe flow Experiments). The test facility and its components are presented in Figure 2. The water flows upwards within the pipe, and there is also an air injector to generate the two-phase flow (Figure 3). The design of the air injector was adapted from the SUBFLOW test facility [2]. Now, three air/water injectors (OD 6 mm, ID 4 mm) were used in a triangular array (side 25 mm) and the air capillaries were slightly larger than in the SUBFLOW (OD 2 mm, ID 1 mm). By adjusting the air and the secondary water flow rates, the initial size of the air bubbles, departing from the air injector, can be varied. If the secondary water flow rate is increased, the air bubbles are departing more frequently from the capillary outlets, hence the bubbles get smaller.

In addition to the axial WMS, the test facility is also equipped with the two traditional cross-sectional wire-mesh sensors (two 32×32 sensors). Two WMSs are typically used together with the small distance in the flow direction for the estimation of the velocities of the gas bubbles as the data can be evaluated using the cross-correlation methods. The Figure 1 shows two example frames from the void fraction measurements previously performed in the HIPE. Later on, these WMSs will be used to study the intrusiveness of the axial WMS. However, the comparative measurements are not yet available to be presented and discussed in this paper.

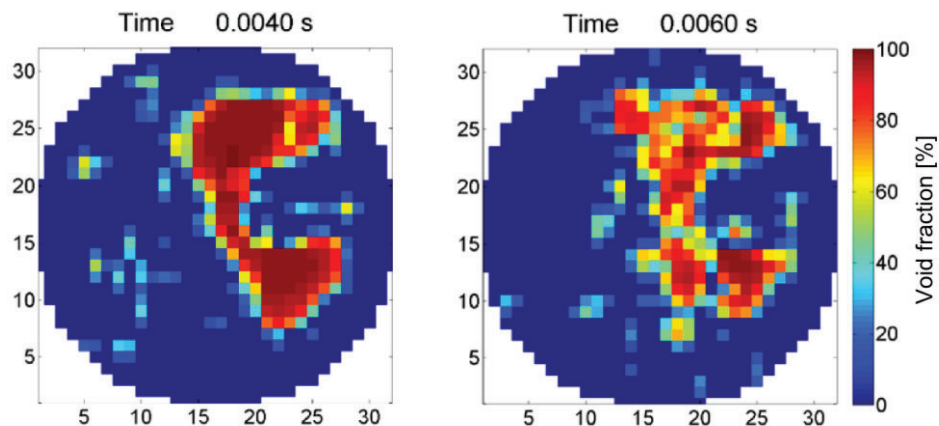


Figure 1. Example frames from the WMS void fraction measurements (Air-Water experiments in the HIPE test facility), 32×32 WMS.

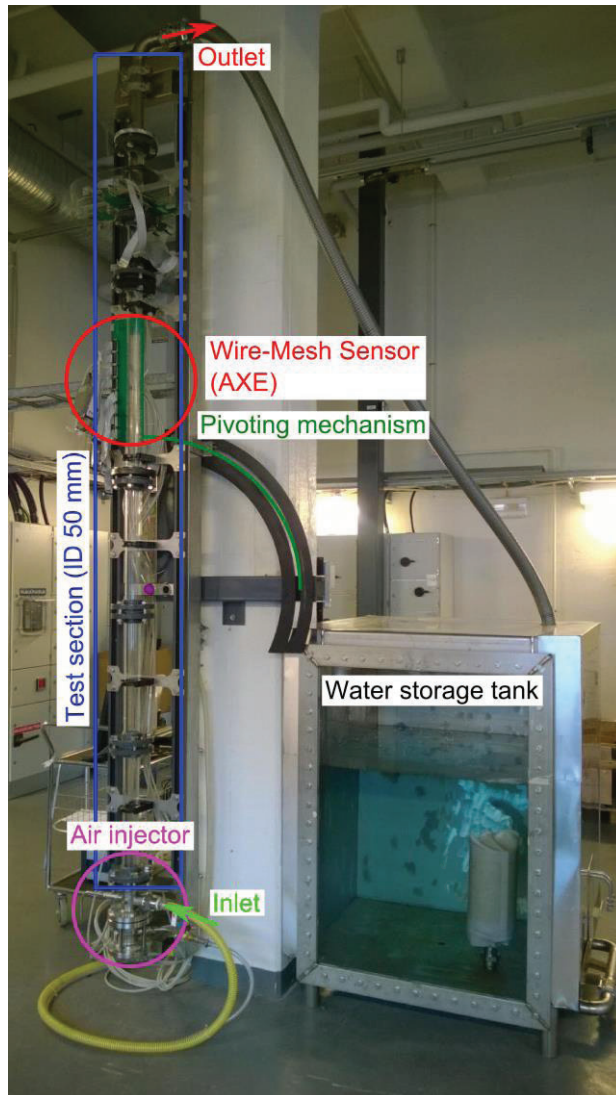


Figure 2. The HIPE test facility (=Horizontal and Inclined Pipe flow Experiments).

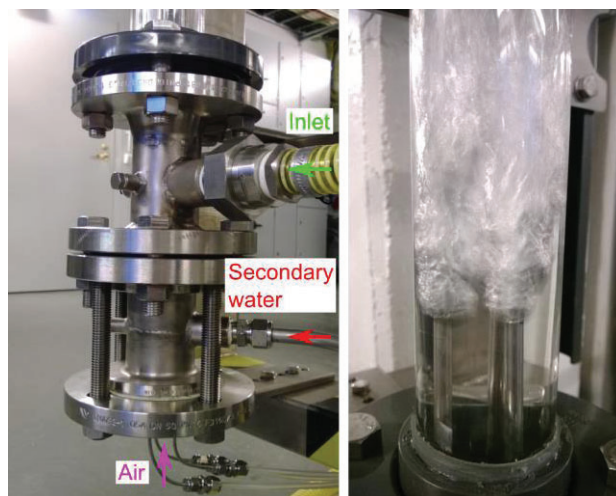


Figure 3. The detailed view of the air injector: The locations of the air and the water inlets (left) and the air bubbles departing from the injector pipes (right).

2.2. The Axial Wire-Mesh Sensor (AXE)

In parallel to the use of the traditional wire-mesh sensors, new applications for the WMS technique have been actively studied. A new type of WMS was designed and constructed in LUT. The design of the sensor is illustrated in Figure 4 and the overview of the sensor during the experiments is presented in Figure 5. The upstream end of the sensor (the left side, in Figure 4) was designed significantly leaner (width 8 mm) than the downstream end (the right side), which is used for the transmitter signal routing. This was done to reduce the flow disturbances produced by the sensor. In addition, a gap of 10 mm was left between the sensor board and the first receiver wire. Like the name of the sensor states, it is installed axially into the centerline of the flow channel to study the axial flow dynamics of the two-phase flow. Typically, WMSs are installed over the cross-section of the flow channel and hence it will be essential to study how this type of axial sensor affects the flow distribution and behavior.

The sensor (16×128 wires, $3 \text{ mm} \times 3 \text{ mm}$ spatial resolution over the area of $45 \times 381 \text{ mm}^2$) is constructed from a standard two-sided Printed Circuit Board (PCB). The essential design parameters are presented in Table I. Some structural problems were studied before the soldering of the stainless steel wires. These included the machining of the Acrylic pipe for the sensor installation and finding out a suitable glue (2-component Epoxy) for fixing the PCB to the channel. During the soldering process some problems were encountered with the loss of tension on the previously soldered wires as the fiberglass PCB had started to bend. This type of unwanted behavior can be avoided by using an additional mounting frame that keeps the PCB of the sensor perfectly flat during the soldering process and once all the wires have been soldered, it can be removed.

The structure of the sensor installation has some advantages and disadvantages. The sealing of the sensor is simple as the gaps between the Acrylic plastic and the PCB are filled with the glue. However, as the wires of the sensor cannot be repaired or thoroughly cleaned after the PCB has been glued to the pipe, they have to be soldered with the utmost care. The structures and the installation can be designed in such a way that the sensor wires could be easily repaired, but it would be difficult in the terms of the sealing.

Table I. The design parameters of the Axial Wire-Mesh Sensor

The Axial Wire-Mesh Sensor (AXE)	
Spatial resolution	3 mm × 3 mm
Temporal resolution	10 000 frames/s
The size of the WMS	16 × 128 wires
The size of the WMS (in mm)	45 × 381 mm ²
The thickness of the wires	0.1 mm
The thickness of the PCB (i.e. The wire layer distance)	1.6 mm

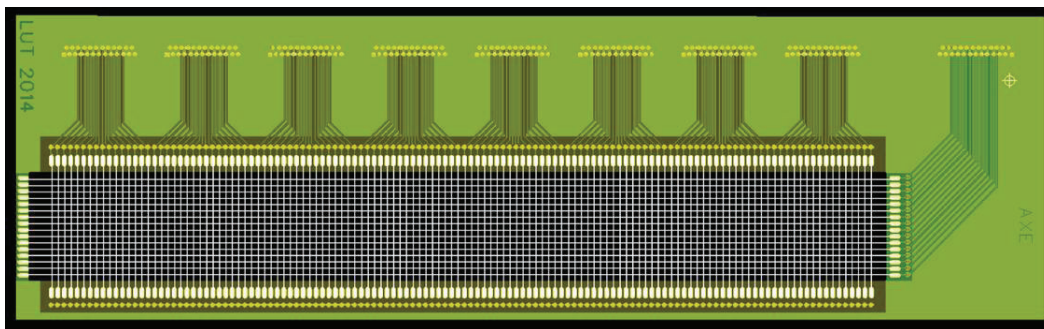


Figure 4. The Axial Wire-Mesh Sensor (AXE).

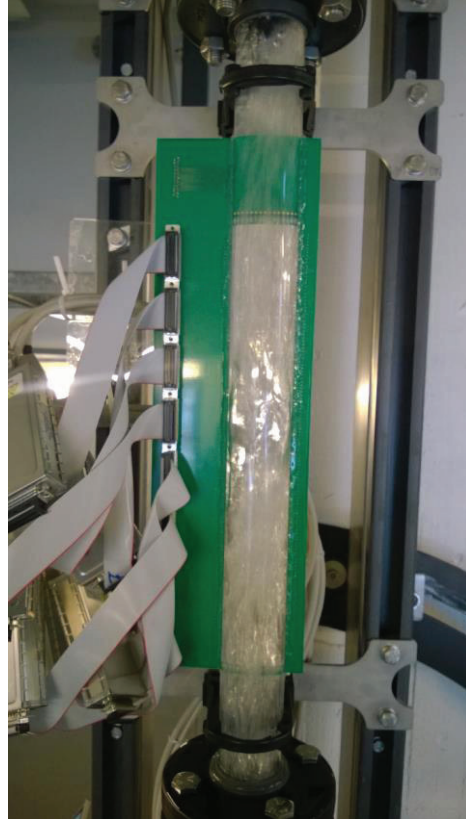


Figure 5. The sensor during the two-phase flow experiments in the HIPE test facility.

3. EXPERIMENTAL RESULTS

A series of two-phase flow experiments was conducted to study the performance of the axial wire-mesh sensor (AXE). The sensor was installed 1540 mm downstream from the air injector outlets (appr. 31 hydraulic diameters). The secondary water flow through the air injector was set zero and the flow channel was aligned in the vertical direction (upward two-phase flow) to reduce the number of the flow variables. The test matrix of the conducted two-phase flow experiments is presented in Table II.

Table II. The test matrix of the HIPE two-phase flow experiments

No.	Superficial water flow rate [m/s]	Superficial air flow rate [m/s]
Test_1_1	0.6	0.08
Test_1_2	0.6	0.17
Test_1_3	0.6	0.25
Test_1_4	0.6	0.34
Test_1_5	0.6	0.42
Test_2_1	1.0	0.08
Test_2_2	1.0	0.17
Test_2_3	1.0	0.25
Test_2_4	1.0	0.34
Test_2_5	1.0	0.42

The flow parameters were selected to cover the bubbly and the slug flow regimes. In Test_1_5, the flow could be identified as the churn flow based on the visual observations and the measured data.

3.1. The Conversion of the Measurement Values

The wire-mesh electronic units use 12-bit analog-to-digital converters (ADC), which results in the measurement range of integer values from 0 to 4079 (the values above are reserved by the WMS electronics). The raw measurement data (i.e. electrical conductance) can be converted to the values of the void fraction using the calibration measurement. The values for the liquid phase have to be separated for those of the gas phase in the two-phase measurements. During the experiments, the values for the amplification are adjusted in a way that a noticeable higher baseline level is measured in the presence of de-mineralized water. If the signal value is less than this baseline, some air is connecting the wire layers. The instantaneous void fractions are calculated by assuming linearity from

$$\alpha_{i,j,k} = \frac{I_{W,i,j} - I_{i,j,k}}{I_{W,i,j}} \cdot 100\% \quad (1)$$

where i and j are the x and y indices of the sensor and k is the index of the frame. The $I_{W,i,j}$ is the averaged signal value for the de-mineralized water at the crossing point i,j . The time-averaged void fractions are calculated for all the crossing points i,j from

$$\bar{\alpha}_{i,j} = \frac{1}{n} \sum_{k=1}^n \alpha_{i,j,k} \quad (2)$$

where n is the total number of the measurement frames (i.e. 200 000 frames).

The calibration measurements were carried out from time to time with the single-phase water flow to have the fresh calibration data available for the data conversion. The duration of the calibration measurement was 5 seconds and the duration of each two-phase flow measurement was 20 seconds with 10 kHz measurement frequency (10 000 frames/s).

3.2. Instantaneous Void Fraction Distributions

Samples of instantaneous void fraction distributions are presented in Figures 6 and 7. The experiments with the different superficial water flow rates are presented separately.

Some interesting observations can be made from the instantaneous void fraction distributions. In Figure 6, with the lowest air flow rate, some quite sizeable bubbles are present on the sensor. In addition, some smaller bubbles are visible in the data. As the air flow rate is increased ($J_G=0.17$ m/s), the slug flow is formed and the data shows large air bubbles that are filling most of the channel diameter. Now, the smaller bubbles are visible in the wake of the larger bubble. As the air flow rate is further increased, the shape of the large air bubbles becomes more distorted ($J_G=0.25$ m/s and 0.34 m/s). With the highest air flow rate ($J_G=0.42$ m/s), the flow could be identified as the churn flow based on the visual observations and the measured data. The large air slugs are extremely distorted and elongated with the twisting gas-liquid interface. The numerous smaller gas bubbles are travelling between the larger distorted slugs.

In Figure 7, the similar behavior can be observed with some differences. As the superficial water flow rate is now higher, the air bubbles are now smaller compared to the measurement with the same air flow rate in Figure 6. Also, the flow with the highest air flow rate is still in the slug flow region and the churn behavior cannot be observed from the data. Some wake bubbles can be noticed near the lower edge of the sensor. The effect of these wake bubbles will be discussed in the next section where their existence is more evident in the data.

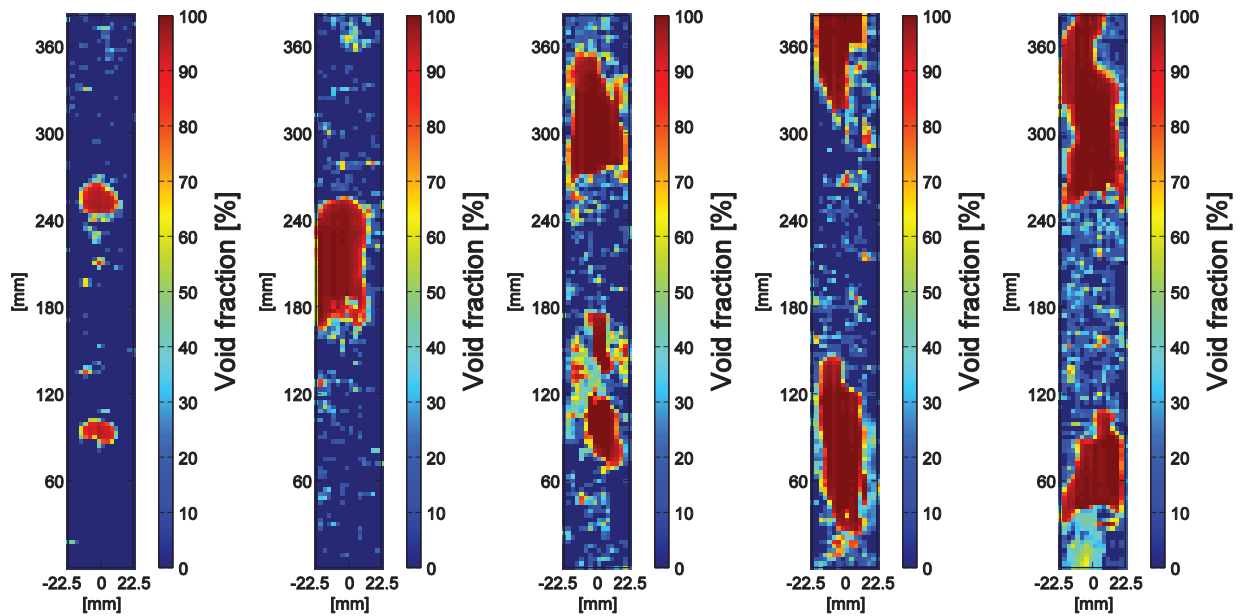


Figure 6. Instantaneous void fraction distributions with $J_L=0.6$ m/s and $J_G=0.08, 0.17, 0.25, 0.34$ and 0.42 m/s (from left to right).

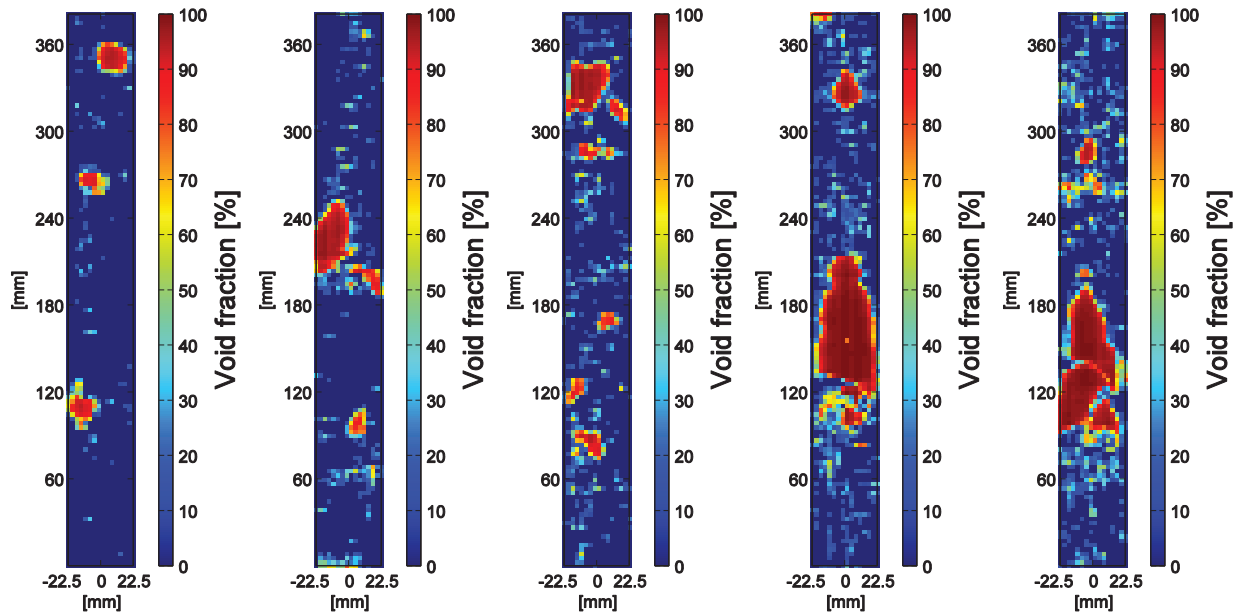


Figure 7. Instantaneous void fraction distributions with $J_L=1.0$ m/s and $J_G=0.08, 0.17, 0.25, 0.34$ and 0.42 m/s (from left to right).

3.3. Time-Averaged Void Fraction Distributions

Time-averaged void fraction distributions are presented in Figures 8 and 9. Some sensor design related observations can be made from the Figures.

The first observation is valid for all the experiments presented in this paper, some distance is needed for the two-phase flow to recover its original form. This can be observed from the void fraction distributions near the lower edge of the sensor. The highest void fraction values are significantly lower than those measured downstream on the sensor as the air bubbles have to go around the lower edge of the sensor where the transmitter wires are fixed (1.6 mm thick and 8 mm in the flow direction). This behavior seems to be more evident as the water and air flow rates are decreased. However, the void fraction profile recovers quite shortly after to its original state (20th receiver wire, 60 mm) and remains quite constant for the rest of the sensor. Some changes can be observed, but to judge whether if it is due to the natural development of the flow or due to the disturbances of the sensor, the comparative measurements with the traditional WMSs are needed.

As mentioned in the previous section, some wake bubbles near the lower edge of the sensor are visible in the data. The presence of the bubbles becomes more evident in the time-averaged void fraction distributions. As the liquid flow rate is increased, the wake bubble effect is more visible. It might be that with the lowest air flow rate, the wake effect is the reason for the slightly asymmetric void fraction distribution through the whole sensor. One could reduce the wake effect by redesigning/machining the lower edge of the sensor PCB.

To summarize, the axial sensor performs well, but the design has some noticeable effects on the flow that have to be recognized when analyzing the data. The axial alignment of the sensor offers new ways to study the flow, but first the numerical tools have to be developed as the algorithms used with the traditional wire-mesh sensor data are not any more valid.

3.4. Applications for the Axial Sensor

If the axial development of the flow is of interest, the axial wire-mesh sensor might give the means to analyze the flow behavior in detail. However, the sensor should be designed such that it would disturb the flow as little as possible. This can be achieved by optimizing the lower edge of the sensor and selecting the best design based on the comparative measurements with the traditional wire-mesh sensors. One possible application for the axial sensor is the study of the swirling devices, which could be now optimized based on the axial measurements.

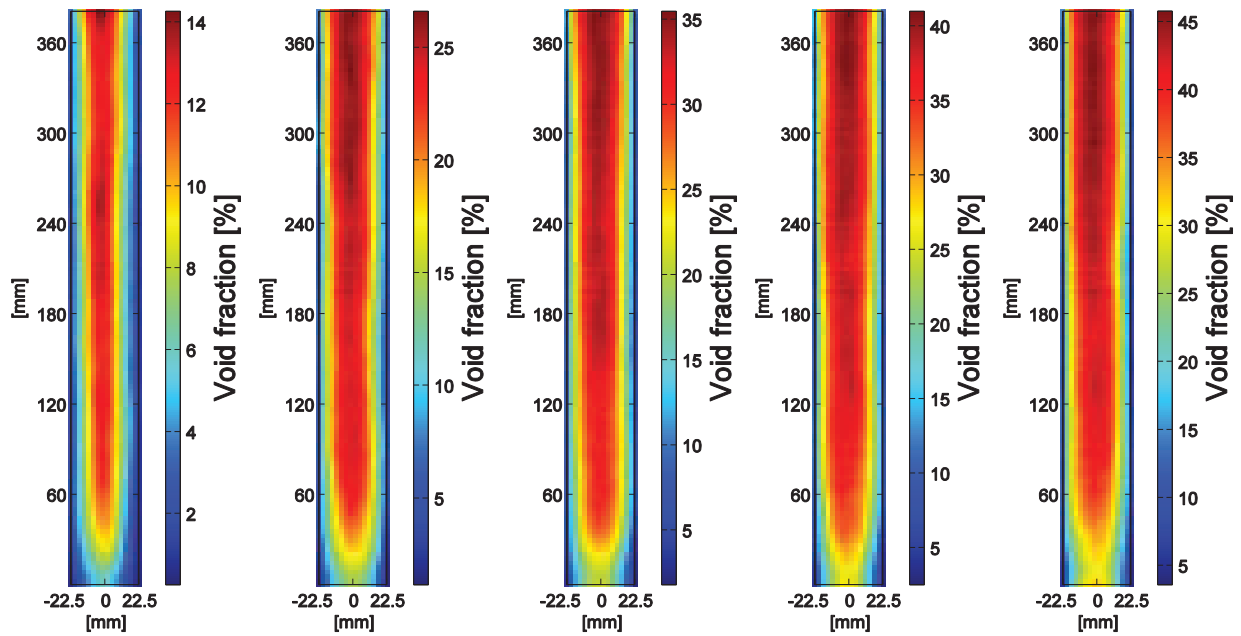


Figure 8. Time-averaged void fraction distributions with $J_L=0.6$ m/s and $J_G=0.08, 0.17, 0.25, 0.34$ and 0.42 m/s (from left to right).

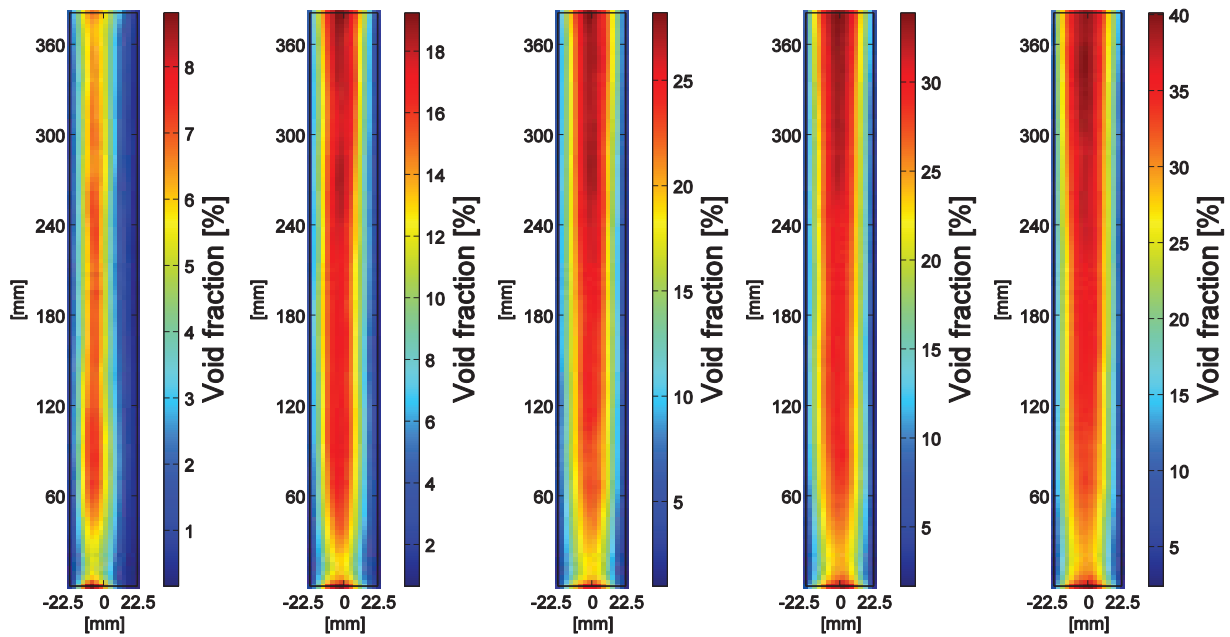


Figure 9. Time-averaged void fraction distributions with $J_L=1.0$ m/s and $J_G=0.08, 0.17, 0.25, 0.34$ and 0.42 m/s (from left to right).

4. CONCLUSIONS

The wire-mesh sensor to study the axial development of the pipe flow was successfully developed and tested in the HIPE test facility. The first results show that the sensor performs well in general, but the design has some disadvantages which were recognized from the data. Despite of its flaws, the sensor offers a new tool for the two-phase flow studies. High temporal and good spatial resolutions enable the study of the flow dynamics in high detail. The “AXE-type” sensor could be used to optimize the design of the swirling devices. The experimental campaign will be continued with an inclined pipe experiments and the comparative experiments with the traditional wire-mesh sensors. In addition, the new numerical data analysis tools will be developed to extract the physical parameters of interest from the data.

ACKNOWLEDGMENTS

The authors wish to acknowledge the funding for the development of the sensor that was provided via The Finnish Research Programme on Nuclear Power Plant Safety 2011 – 2014 (SAFIR2014).

REFERENCES

1. H.-M. Prasser, A. Böttger, and J. Zschau, “A new electrode-mesh tomography for gas-liquid flows,” *Flow Measurement and Instrumentation*, **9**(2), pp. 111-119 (1998).
2. A. Ylönen and H.-M. Prasser, “Two-phase flow and cross-mixing measurements in a rod bundle,” *Proceedings of The 14th International Topical Meeting on Nuclear Reactor Thermalhydraulics (NURETH-14)*, Toronto, Canada, September 25-30, 2011.
3. A. Ylönen and H.-M. Prasser, “Flow mixing experiments with spacer grids in a 4×4 rod bundle,” *Proceedings of The 15th International Topical Meeting on Nuclear Reactor Thermalhydraulics (NURETH-15)*, Pisa, Italy, May 12-17, 2013.
4. M. Damsohn and H.-M. Prasser, “High-speed liquid film sensor for two-phase flows with high spatial resolution based on electrical conductance,” *Flow Measurement and Instrumentation*, **20**(1), pp. 1-14 (2009).
5. M. Ritterath, O. C. Öztürk, and H.-M. Prasser, “Thermo-resistive mesh sensors (TMS) for temperature field measurements,” *Flow Measurement and Instrumentation*, **22**(4), pp. 343-349 (2011).
6. D. Bertolotto, *Coupling a System Code with Computational Fluid Dynamics for the Simulation of Complex Coolant Reactivity Effects*, PhD thesis (no. 5227), EPFL, Lausanne, Switzerland (2011).
7. S. Kliem, T. Sühnel, U. Rohde, T. Höhne, H.-M. Prasser, F.-P. Weiss, “Experiments at the mixing test facility ROCOM for benchmarking of CFD-codes,” *Proceedings of CFD4NRS workshop*, Garching, Munich, Germany, September 5-7, 2006.